

Particle filter source tracking in an uncertain environment

Caglar Yardim, Peter Gerstoft, and William S. Hodgkiss

*Marine Physical Laboratory,
Scripps Institution of Oceanography,*

La Jolla,

California 92093-0238

(email: cyardim@ucsd.edu,

gerstoft@ucsd.edu,

whodgkiss@ucsd.edu)

(Dated: March 24, 2009)

Abstract

Abstract: This paper addresses the tracking of acoustic source parameters such as depth, range and speed in spatially and temporally changing ocean acoustic environments. Conventional matched-field processing requires an accurate knowledge of environmental parameters (e.g. sound speed profile (SSP), water depth, sediment and bottom parameters) for source localization. Since environmental mismatch may result in significant errors in source parameters, algorithms that minimize this mismatch should be employed. For this purpose, a particle filtering (PF) approach is adopted here where the geoacoustic parameters are tracked simultaneously with the source location and ship speed in a range-dependent environment. This allows real-time updating of the environment and accurate tracking of the moving source. As a sequential Monte Carlo technique that operates on nonlinear systems with non-Gaussian probability densities, the PF is an ideal algorithm to perform tracking of source and environmental parameters, and their uncertainties via the evolving posterior probability densities. The algorithm is demonstrated on simulated data in a sloping bottom environment with SSP, water depth and sediment parameters evolving as the ship moves.

PACS numbers: 43.30.Pc, 43.60.Pt, 43.60.Wy

I. INTRODUCTION

Passive localization and tracking of a moving source are important problems in ocean acoustics. Matched-field processing (MFP) has been applied successfully to source localization and tracking problems by finding the best match between measured and simulated acoustic fields using a forward model such as a normal mode or a parabolic equation code at an assumed source location¹⁻¹⁸. MFP works well in multipath environments including the complicated interaction between the water column and sedimentary layers. The important parameters that describe the ocean environment acoustically include the water column sound speed profile (SSP) and sedimentary layer properties such as the thicknesses, sound speeds, attenuation, and densities. The selection of environmental parameters that affect significantly source tracking depends on several factors such as the measurement setup and frequency¹⁴. Lower frequency MFP needs to take into account deeper sedimentary layers but may be less affected by fluctuations in the water column SSP, whereas high frequency tracking will be influenced more by shallow sedimentary layers and fluctuations in the SSP.

MFP needs an accurate representation of the environment in order to localize and track the source. The sensitivity of classical MFP to environmental mismatch has been well-studied¹⁹, *e.g.* sensitivity to errors in SSP²⁰ and effects of water depth mismatch^{21,22}. Often, these environmental parameters are not known a priori.

Some of the strategies that have been adopted to increase the robustness of MFP source localization to an unknown environment include the optimum uncertain field processor¹ (OUFP) and focalization². Focalization deals with the source localization problem in an unknown environment by including environmental parameters as unknown inversion parameters along with the source parameters and optimizing the parameters using global search techniques. This technique eliminates the environmental mismatch but the search space is increased due to the addition of new variables. The OUFP marginalizes over the environmental parameters using a prior to obtain the posterior probability density (PPD) of the source parameters. This method effectively averages the source location over all envi-

ronments, making the MFP source localization robust to environmental uncertainty. This approach also provides for a PPD, hence information about the uncertainty in the estimates. Extended Kalman filters also have been used for source localization⁶.

Tracking can be achieved by using one of the localization techniques mentioned above successively as the source moves. This approach is referred to as the conventional tracking algorithm (CTA). A better alternative to CTA is using a motion based tracking algorithm (MBTA) which incorporates into the tracking algorithm information about the source movement. The optimum uncertain field tracking algorithm⁹ (OUFTA) is such an extension of the OUFP. By examining the whole sequence of data and assuming a constant environment with a given prior probability density function (PDF), the OUFTA computes the most likely source path using a Viterbi algorithm by integrating out the uncertain environment. This method does not quantify the uncertainty in the source location. Another MBTA given in Ref. 17 uses the entire data sequence to track the source in an unknown but constant environment. One difference between this method and OUFTA is that the unknown environment is also estimated along with the source locations. The source locations at different time steps are treated as separate parameters and are estimated along with the environmental parameters in one big inversion step that include all the data. Since the dimension of the search space increases (often by 2) with each new data point and source location, the technique requires an efficient sampling technique.

Many of the algorithms that deal with source tracking in uncertain environments assume a constant environment. However, tracking involves a moving source and hence the ocean environment and the path between the source and receiver is changing with both space and time. Therefore, a particle filtering (PF) approach is adopted here to track both the source and environmental parameters. It also is a MBTA, however, the source model is flexible and easily can be modified. A constant velocity (CV) model is used here. The acceleration error term enables the algorithm to adapt to accelerating/decelerating sources.

Previous studies show that the PF is very versatile and robust in tracking environmental changes in both acoustic²³ and electromagnetic²⁴ applications. It also has been shown that

a geoacoustic PF with enough particles can attain a mean square error very close to the posterior Cramér-Rao lower bound that provides a limit on the achievable track performance²³. Therefore, these techniques can be merged with source tracking algorithms to achieve real-time source tracking in changing ocean environments. This enables us to track both source parameters such as speed, range and depth along with environmental parameters.

Since the PF is an evolving set of particles, with each particle representing a possible solution, the evolving PPD also is tracked enabling the PF to track the evolving uncertainty in the parameter estimates. Due to the availability of the PPD at each step, it is possible to pick the best particle at each time step as a maximum a posteriori solution (similar to focalization) or it is possible to integrate out the environmental parameters by marginalization (similar to OUPF). The effects of focalization and marginalization are discussed in detail in Ref. 25.

II. THEORY

Geoacoustic tracking requires two dynamic equations²³: A state equation that models the evolution of the environment and movement of the source, and an acoustic measurement equation that relates the environment and the source location at step k to the acoustic field measured across the receiver array. These are given as

$$\mathbf{x}_k = \mathbf{F}_{k-1}\mathbf{x}_{k-1} + \mathbf{B}_{k-1}\mathbf{v}_{k-1} \quad (1)$$

$$\mathbf{y}_k = \mathbf{h}(\mathbf{x}_k) + \mathbf{w}_k = a_k\mathbf{d}(\mathbf{x}_k) + \mathbf{w}_k \quad (2)$$

where \mathbf{F} is a known linear function of the state vector \mathbf{x}_{k-1} , and $\mathbf{h}(\cdot)$ is the nonlinear function that relates the environmental and source parameters \mathbf{x}_k to the acoustic measurement vector \mathbf{y}_k . Hence, $\mathbf{h}(\cdot)$ includes both the unknown source amplitude term a_k and the known forward model $\mathbf{d}(\mathbf{x}_k)$. \mathbf{v}_k , \mathbf{w}_k , and \mathbf{B}_k are the process/state noise vector, the measurement noise

vector, and the scaling matrix, respectively with

$$\begin{aligned}
\mathbb{E}\{\mathbf{v}_k \mathbf{v}_i^T\} &= \mathbf{Q}_k \delta_{ki} \\
\mathbb{E}\{\mathbf{w}_k \mathbf{w}_i^T\} &= \mathbf{R}_k \delta_{ki} \\
\mathbb{E}\{\mathbf{v}_k \mathbf{w}_i^T\} &= \mathbf{0} \quad \forall i, k,
\end{aligned} \tag{3}$$

where \mathbf{Q}_k and \mathbf{R}_k are the covariance matrices at k for the corresponding noise terms.

A. The State Equation: Ocean and Acoustic Source Modeling

The state equation is formed from two blocks. The first one includes the state equation needed for source tracking. The three source parameters (*i.e.* the source depth, range, and radial speed) are grouped as $\mathbf{s}_k = [z_s \ r_s \ v_s]_k^T$. Using a constant velocity (CV) track model for the source, the first block in the state equation is given by:

$$\begin{aligned}
\mathbf{s}_k &= \mathbf{F}_{k-1}^s \mathbf{s}_{k-1} + \mathbf{B}_{k-1}^s \mathbf{v}_{k-1}^s, \tag{4} \\
\begin{bmatrix} z_s \\ r_s \\ v_s \end{bmatrix}_k &= \begin{bmatrix} 1 & 0 & 0 \\ 0 & 1 & \Delta t \\ 0 & 0 & 1 \end{bmatrix} \begin{bmatrix} z_s \\ r_s \\ v_s \end{bmatrix}_{k-1} + \begin{bmatrix} 1 & 0 \\ 0 & \frac{\Delta t^2}{2} \\ 0 & \Delta t \end{bmatrix} \begin{bmatrix} v_{z_s} \\ v_{a_s} \end{bmatrix}_{k-1}, \tag{5}
\end{aligned}$$

where Δt is the time between successive measurements, v_{z_s} and v_{a_s} are random variables representing the variation in source depth and acceleration, respectively. The PF allows for any type of PDFs to be used for these two variables. However, zero-mean Gaussian random variables are appropriate for the setup used in this paper.

The PF framework is very versatile and other source models can be used depending on the application. The CV model can be replaced with a fixed source model where only depth and range are state variables and speed is included only indirectly as a noise term (similar to the acceleration term used in the CV model) to mitigate the effects in case the source moves. Similarly for more complicated moving targets, a full moving source model can be used where the depth, range, speed, and acceleration are state variables. Unlike the ship-towed source used here, the source also could move in depth. Then the model simply

is replaced by one which includes the vertical speed and/or acceleration in addition to the range parameters. In scenarios where it is possible to extract information about the azimuth of the source (*e.g.* a horizontal receiver array) it is possible to replace the above models with a 2-D motion model. Finally, it also is possible to include more than one of these models and employ a multiple model particle filter²⁶.

The second block is the state equation for the environmental parameters. The environmental parameters such as the SSP and sediment parameters, water depth at step k are grouped into \mathbf{m}_k . The same environmental evolution model given in Ref. 23 is used. This model assumes that the rate of change of the environment is slow relative to step index k . Hence, the second block is given by

$$\mathbf{m}_k = \mathbf{F}_{k-1}^{\mathbf{m}} \mathbf{m}_{k-1} + \mathbf{B}_{k-1}^{\mathbf{m}} \mathbf{v}_{k-1}^{\mathbf{m}}, \quad (6)$$

with $\mathbf{F}^{\mathbf{m}} = \mathbf{B}^{\mathbf{m}} = \mathbf{I}$ where \mathbf{I} is the identity matrix, and $\mathbf{v}^{\mathbf{m}}$ is the state noise matrix for the environmental parameters that takes into account the error in the evolution model. Even though many geoacoustic parameters are expected to be evolving slowly most of the time, there can be sudden jumps at the boundaries of geological formations, violating the evolution model selected here. To continue tracking the parameters successfully through the sudden jump, the geoacoustic tracking filters will have to incorporate a state noise term $\mathbf{v}^{\mathbf{m}}$ with a high covariance \mathbf{Q}_k .

The initial density $p(\mathbf{m}_0)$ ideally can be obtained by running a Markov chain Monte Carlo geoacoustic inversion at $t = 0$. Since the PF can operate on nonlinear densities, any type of PDF can be used. In practical cases, the tracking algorithms can be coupled with a standard geoacoustic inversion algorithm^{1-8,15,16,18,27} that inverts for the environment and source location at $t = 0$ to supply $p(\mathbf{x}_0)$.

The state vector that includes both the source and the environmental parameters is given by merging these two blocks. Defining the state vector as $\mathbf{x}_k^{\mathbf{T}} = [\mathbf{s}_k^{\mathbf{T}} \ \mathbf{m}_k^{\mathbf{T}}]$, the state

equation is obtained by inserting Eqs. (4) and (6) into Eq. (1):

$$\begin{bmatrix} \mathbf{s} \\ \mathbf{m} \end{bmatrix}_k = \begin{bmatrix} \mathbf{F}_{k-1}^s & 0 \\ 0 & \mathbf{I} \end{bmatrix} \begin{bmatrix} \mathbf{s} \\ \mathbf{m} \end{bmatrix}_{k-1} + \begin{bmatrix} \mathbf{B}_{k-1}^s & 0 \\ 0 & \mathbf{I} \end{bmatrix} \begin{bmatrix} \mathbf{v}^s \\ \mathbf{v}^m \end{bmatrix}_{k-1} \quad (7)$$

Note that in a CTA that runs successive, independent geoacoustic inversions, there is no environmental evolution/source motion model (state equation, Eq. (1)). Therefore, there is no equivalent of the state noise term \mathbf{v}_k in those algorithms. \mathbf{v}_k is an indicator of how much we should trust the previous location and the evolution/motion model itself, representing the error or deviations from the evolution model. A changing water depth when the environment is assumed to be the same at the next time step or an accelerating source in a CV model are two examples of this process. Hence, \mathbf{v}_k is used to make the PF robust in the event that there are unexpected changes in parameter values that are not already included in the evolution model.

B. The Measurement Equation: Acoustic Propagation Model

The measurement equation given in Eq. (2) relates the environmental and source model parameters to acoustic measurements. The acoustic field across the receiver array in a range-dependent environment is calculated by SNAPRD^{27,28} based on adiabatic normal modes assuming the change is gradual. If there are strong variations that cannot be handled by the adiabatic normal mode code, a parabolic equation code can be used instead. For a given state vector \mathbf{x} , the acoustic field is computed by passing the environmental and source parameters (except source speed) to the SNAPRD code.

III. GEOACOUSTIC PARTICLE FILTER

The particle filter is a sequential Monte Carlo method that is used to track desired parameters and their underlying PDFs as they evolve both in space and time²⁹. PFs work well in tracking geoacoustic parameters²³ due to their ability to handle highly nonlinear

systems with non-Gaussian densities. Following Ref. 23, a sequential importance resampling (SIR)³⁰ type PF is adopted here.

The SIR algorithm uses a set of n_p particles $\{\mathcal{X}_k^i\}_{i=1}^{n_p}$ to represent the PDF at each step k . The filter has predict and update sections which the SIR filter uses first for predicting the next set of values of the environmental and source parameters given their previous history and then including the latest measurement result to correct/update the predicted value and their PDFs. The initial set of particles $\{\mathcal{X}_0^i\}_{i=1}^{n_p}$ are sampled from the prior $p(\mathbf{x}_0)$. The SIR filter uses the importance sampling³¹ density as the transitional prior $p(\mathbf{x}_k|\mathbf{x}_{k-1})$. Although this is a suboptimal choice, it is easy to sample from this density. This selection results in particle weights proportional to the likelihood $W_k \propto p(\mathbf{y}_k|\mathbf{x}_k)$. In geoacoustic tracking the complex source amplitude a_k usually is not known. Therefore, this term is estimated with a ML estimator during the likelihood calculation of each particle in the ensemble³². A more detailed discussion about the effects of this selection on source localization can be found in Ref. 33. The likelihood function for the i th particle at step k can be written as

$$\mathcal{L}(\mathcal{X}_{k|k-1}^i) = p(\mathbf{y}_k|\mathcal{X}_{k|k-1}^i) = \prod_{j=1}^{n_f} \frac{1}{\pi^{n_h} |\mathbf{R}_k^j|} \exp[-\phi_k^{ij}], \quad (8)$$

$$\phi_k^{ij} = [\mathbf{y}_k^j - a_k^{ij} \mathbf{d}^j(\mathcal{X}_{k|k-1}^i)]^H (\mathbf{R}_k^j)^{-1} [\mathbf{y}_k^j - a_k^{ij} \mathbf{d}^j(\mathcal{X}_{k|k-1}^i)], \quad (9)$$

where n_h is and n_f are the number of hydrophones and the frequencies used in tracking, ϕ_k^{ij} and \mathbf{y}_k^j are the cost function and the acoustic field across the array for the j th frequency, and \mathbf{R}_k^j is the measurement noise covariance defined in Eq. (3). Assuming that the complex Gaussian noise \mathbf{w}_k is uncorrelated with same variance along the array ($\mathbf{R}_k^j = \nu_k^j \mathbf{I}$),

$$\mathcal{L}(\mathcal{X}_{k|k-1}^i) = \prod_{j=1}^{n_f} \frac{1}{(\pi \nu_k^j)^{n_h}} \exp\left(-\frac{\|\mathbf{y}_k^j - a_k^{ij} \mathbf{d}^j(\mathcal{X}_{k|k-1}^i)\|^2}{\nu_k^j}\right). \quad (10)$$

The ML estimate for the source a_k^{ij} is then obtained by solving for $\partial \mathcal{L} / \partial a_k^{ij} = 0$, giving

$$\tilde{a}_k^{ij} = \frac{\mathbf{d}^j(\mathcal{X}_{k|k-1}^i)^H \mathbf{y}_k^j}{\|\mathbf{d}^j(\mathcal{X}_{k|k-1}^i)\|^2}. \quad (11)$$

The prediction step consists of sampling from the prior. Then the normalized weight W_k^i of each particle is calculated from its likelihood function. The update step includes the resampling section where a new set of n_p particles is generated from the parent set according to the

weights of the parent particles, with high likelihood particles generating more particles than the low likelihood ones. Hence, a single iteration of the recursive geoacoustic SIR algorithm is summarized as²³:

$$\{\mathcal{X}_{k|k-1}^i\}_{i=1}^{n_p} \sim p(\mathbf{x}_k|\mathbf{x}_{k-1}) \quad (12)$$

$$\mathbf{h}^j(\mathcal{X}_{k|k-1}^i) = \hat{a}_k^{ij} \mathbf{d}^j(\mathcal{X}_{k|k-1}^i) = \frac{\mathbf{d}^j(\mathcal{X}_{k|k-1}^i)^H \mathbf{y}_k^j \mathbf{d}^j(\mathcal{X}_{k|k-1}^i)}{\|\mathbf{d}^j(\mathcal{X}_{k|k-1}^i)\|^2} \quad (13)$$

$$p(\mathbf{y}_k|\mathcal{X}_{k|k-1}^i) = \prod_{j=1}^{n_f} \frac{1}{(\pi\nu_k^j)^{n_h}} \exp\left(-\frac{\|\mathbf{y}_k^j - \mathbf{h}^j(\mathcal{X}_{k|k-1}^i)\|^2}{\nu_k^j}\right) \quad (14)$$

$$W_k^i = \frac{p(\mathbf{y}_k|\mathcal{X}_{k|k-1}^i)}{\sum_{i=1}^{n_p} p(\mathbf{y}_k|\mathcal{X}_{k|k-1}^i)} \quad (15)$$

$$\{\mathcal{X}_{k|k}^i\}_{i=1}^{n_p} = \text{Resample} \left[W_k^l, \{\mathcal{X}_{k|k-1}^l\}_{l=1}^{n_p} \right] \quad (16)$$

$$s.t. \quad \Pr \{ \mathcal{X}_{k|k}^l = \mathcal{X}_{k|k-1}^l \} = W_k^l$$

IV. EXAMPLE

This section is composed of a synthetic source tracking example in a sloping bottom, shallow water environment. The model parameterization includes the water depth, SSP, sediment and bottom parameters, see Fig. 1(a). The model, the starting environmental parameters and the receiver array are inspired by Ref. 17. The geoacoustic parameters include sediment thickness h_{sed} , sound speed, density, and attenuation for both sediment and bottom layers, the water depth at the source location D , and a four-parameter SSP (c_1 - c_4 at depths of 0, 10, 50, and 100 m). Instead of the actual sound speed values, the difference between layer sound speeds are used to reduce the inter-parameter correlation. The state vector includes c_1 , $\Delta c_1 = c_1 - c_2$, $\Delta c_2 = c_2 - c_3$, and $\Delta c_3 = c_3 - c_4$. Water depth at the VLA receiver is 130 m. The environmental parameters, their start values and prior standard deviations (\mathbf{x}_0 and $\mathbf{P}_0^{1/2}$), state noise \mathbf{Q}_k , lower and upper bounds of parameters are given in Table I.

The set-up and the movement of the source are shown in Fig. 1(b). The simulation

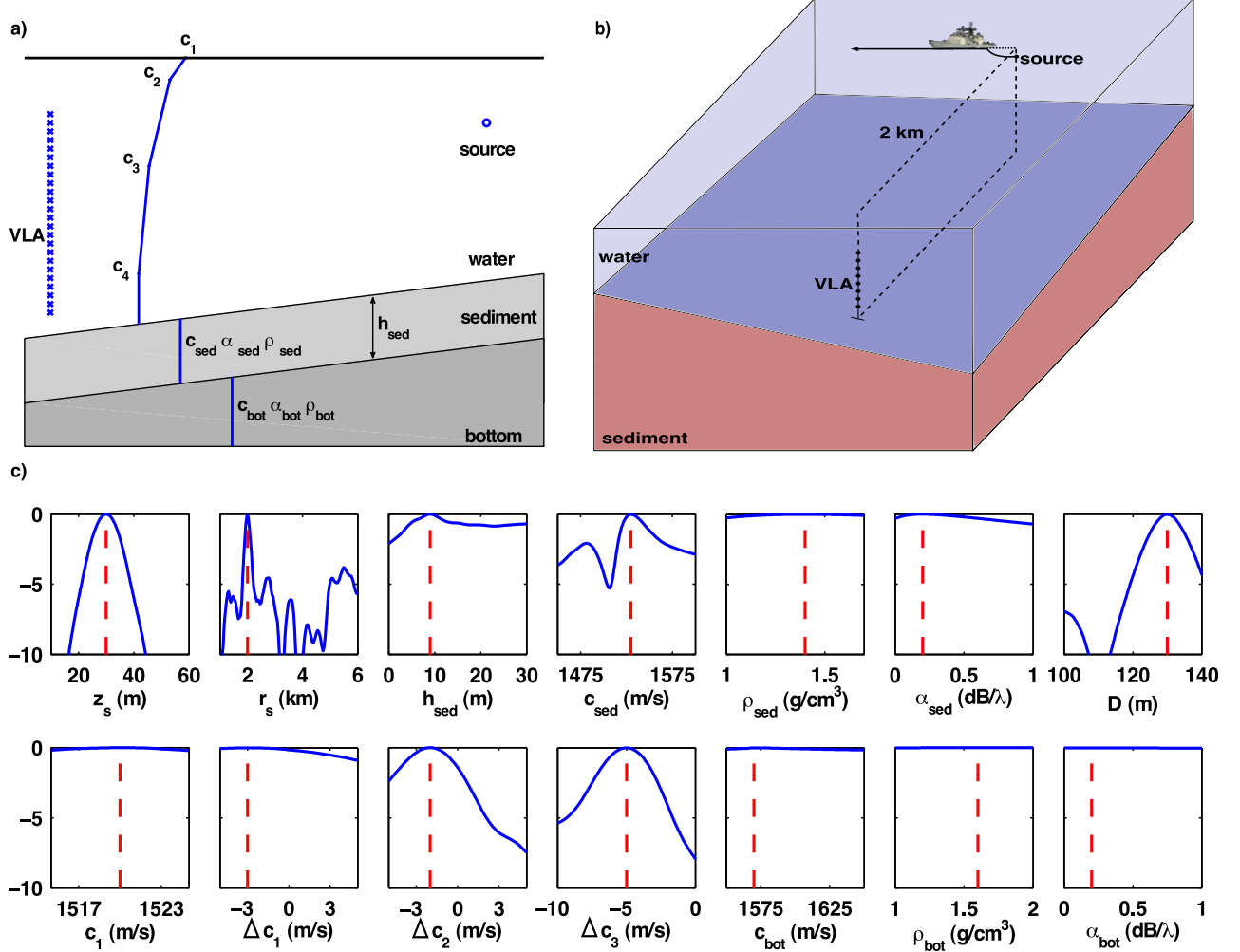


FIG. 1. (Color online) (a) Geoacoustic model used in the simulations, (b) the simulation set-up involving a fixed VLA and moving source in a range-dependent environment, and (c) sensitivity plots of geoacoustic parameters at $t = 0$.

starts at a source range of 2 km with the source moving at a constant velocity of 5 m/s perpendicular to the source-receiver plane. Since the source/receiver is a single element source/VLA set-up, only the radial component of the source velocity can be extracted. The received acoustic field across the VLA contains information about source depth z_s , range r_s , and radial source speed v_s . Since the ship moves perpendicular to the source-receiver plane initially, $v_s = 0$ at $t = 0$, slowly increasing and converging to the full ship velocity of 5

m/s (~ 10 knots) as the ship moves. This results in a large initial radial acceleration, which slowly decreases as the ship moves further away. Therefore, the CV model source evolution formulation in Eq. (5) is not accurate due to the ship's orientation relative to the receiver VLA-source plane. Thus, the acceleration error term v_{a_s} in Eq. (5) will have to compensate for the error in the evolution model. Such an example allows us to study the robustness of PF source tracking when the source evolution model has errors.

The simulations parameters are given in Table II. Four frequencies (200, 275, 350, and 425 Hz) are used with a total track length of 13.3 minutes ($k = 40$) during which the ship travels from 2 to 4.38 km radial range. The element signal to noise ratio (SNR)¹⁷

$$\text{SNR} = 10 \log \frac{[a_k \mathbf{d}(\mathbf{x}_k)]^H [a_k \mathbf{d}(\mathbf{x}_k)]}{\mathbf{w}_k^H \mathbf{w}_k} \quad (17)$$

starts at 8.8 dB at 2 km and decreases with range as shown in Table II. Note that the 24 element array used here will have an array gain of 13.8 dB, giving an array SNR of 22.6 dB at 2 km. The SNR at each frequency is assumed identical, however the algorithm can use different SNR at each frequency and time step.

Water depth at source location (D) starts at 130 m, same as the water depth at the VLA location, and decreases slowly to 100 m as the ship moves. Other environmental parameters and source depth fluctuate as 1st order Markov chains following Eq. (1) with a variance the same as the diagonal elements of \mathbf{Q}_k . A sensitivity analysis is carried out to assess which geoacoustic parameters affect the acoustic field at $t = 0$, see Fig. 1(c). The results show that the field strongly depends on the source parameters, sediment thickness and sound speed, water depth and lower layer SSP parameters, and less on sediment attenuation and upper layer SSP parameters. The acoustic field has very little sensitivity to sediment density. The bottom parameters have little affect on the measured field and are not included in the list of parameters to be tracked.

It is assumed that the initial environment at $t = 0$ has a Gaussian prior PDF with a variance \mathbf{P}_0 given in Table I. Three different simulations are performed on the synthetic data:

1. *Full PF*: A PF that tracks the environmental and source parameters simultaneously.
2. *Mismatched MFP*: Standard matched field processing (MFP) that does not update the changes in the environment and uses the environment at $t = 0$.
3. *Source-only PF*: A PF that tracks only the three source parameters, ignoring the evolution in the environment, similar to the mismatched MFP case.

The results of full PF are given in Figs. 2–5. The evolution of the 1-D marginal posterior densities are given in Fig. 2. The plots in the first row belong to the source parameters. For all three source parameters, the 1-D marginal PPDs follow the true parameter trajectories. Due to the ability of the full PF to correct for the variations in the environment, the source range is tracked with a very low rms error. The source depth PPD becomes multimodal and non-Gaussian at large t where the ship is further from the source resulting in a lower SNR. Variation in the radial source velocity is also well-tracked even with the selected constant velocity evolution model. The environmental parameter tracks are given in the rows 2-4. Many of the PPDs become non-Gaussian and some of the parameters are tracked better than others. Since the SSP (from Ref. 17) is downward refracting, most of the acoustic energy is concentrated in the lower water column, interacting with the sedimentary layer. This is in agreement with the sensitivity curves in Fig. 1(c). The sensitivity of the field to the sound speed c_1 is very low, represented by a flat curve as the acoustic propagation is sensitive to the slope of the SSP, not the absolute value. The PPD becomes less flat as the sound speed index increases with Δc_1 being the least sensitive and Δc_3 being the most because of the refractive profile. The effects of this on the PF performance can be observed directly by comparing the evolving PPDs and their variances. c_1 and Δc_1 are the least well-tracked parameters with highly non-Gaussian PDFs and large variances, whereas Δc_3 is well-tracked at all times with a sharp unimodal density. Δc_2 track lie somewhere between these two cases. This selection of the SSP is also the reason for the high sensitivity to some of the sediment parameters such as h_{sed} due to the heavy acoustical interaction with the top sediment layer. Sound speed in the sediment has a non-Gaussian and a quickly-changing PPD. The sediment density and attenuation also show similar patterns with multimodal

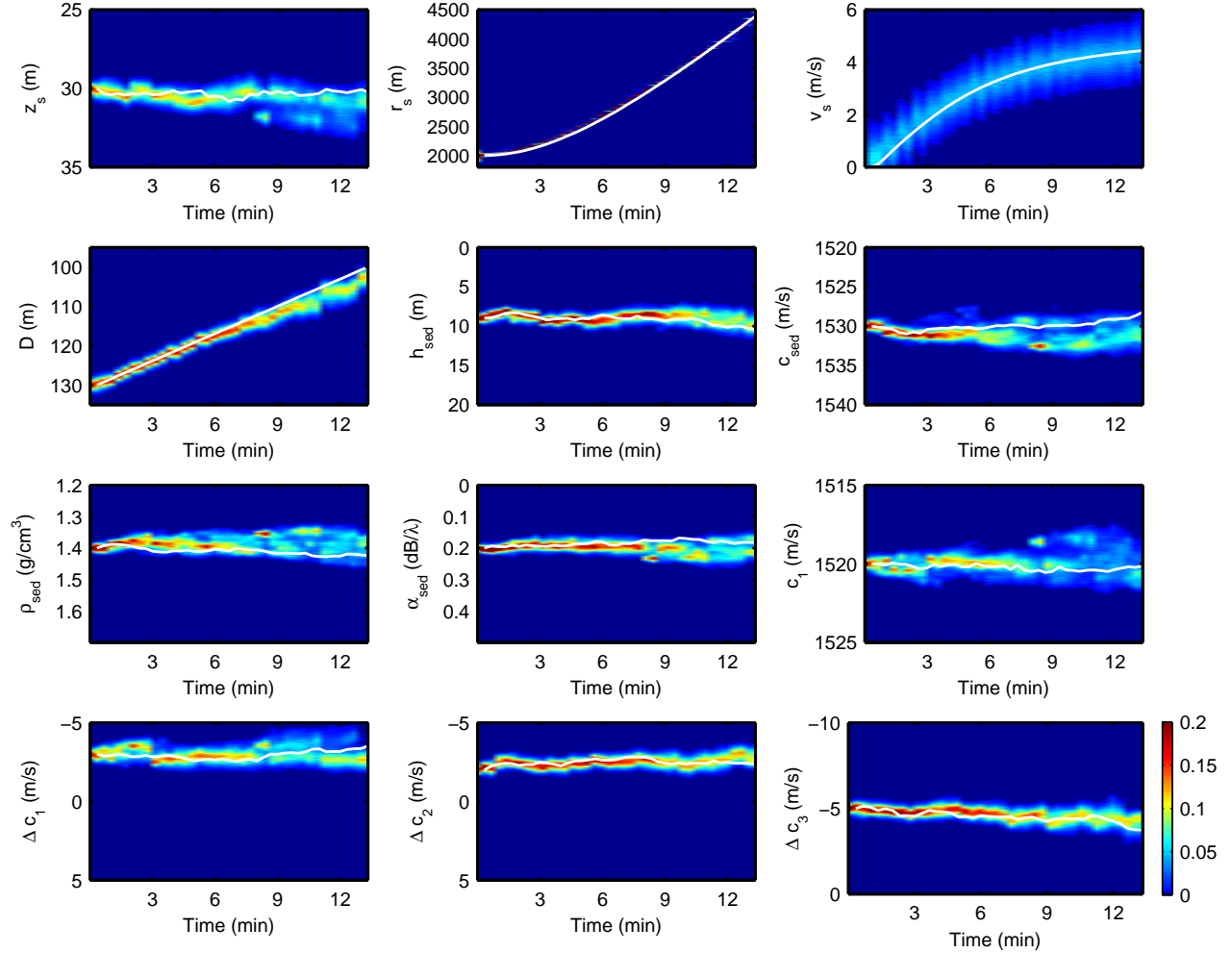


FIG. 2. (Color online) Time evolving marginal posterior density for the full PF simulation and the true trajectory (solid white) of each parameter.

PPDs consistent with their low sensitivity. The PPDs of many of the parameters become wider as t increases due to the decreasing SNR in terms of \mathbf{R}_k .

A vertical slice from each of the evolving PDDs in Fig. 2 is given in Fig. 3 for $t = 10$ min. This snapshot shows better how some parameters such as h_{sed} , v_s , Δc_2 and Δc_3 are tracked more easily than others that are either less sensitive (ρ_{sed} , α_{sed} , c_1) or quickly changing parameters (D). The only environmental parameter that is changing fast is the water depth (D) at the moving source location. Fig. 2 shows that D is tracked well enough

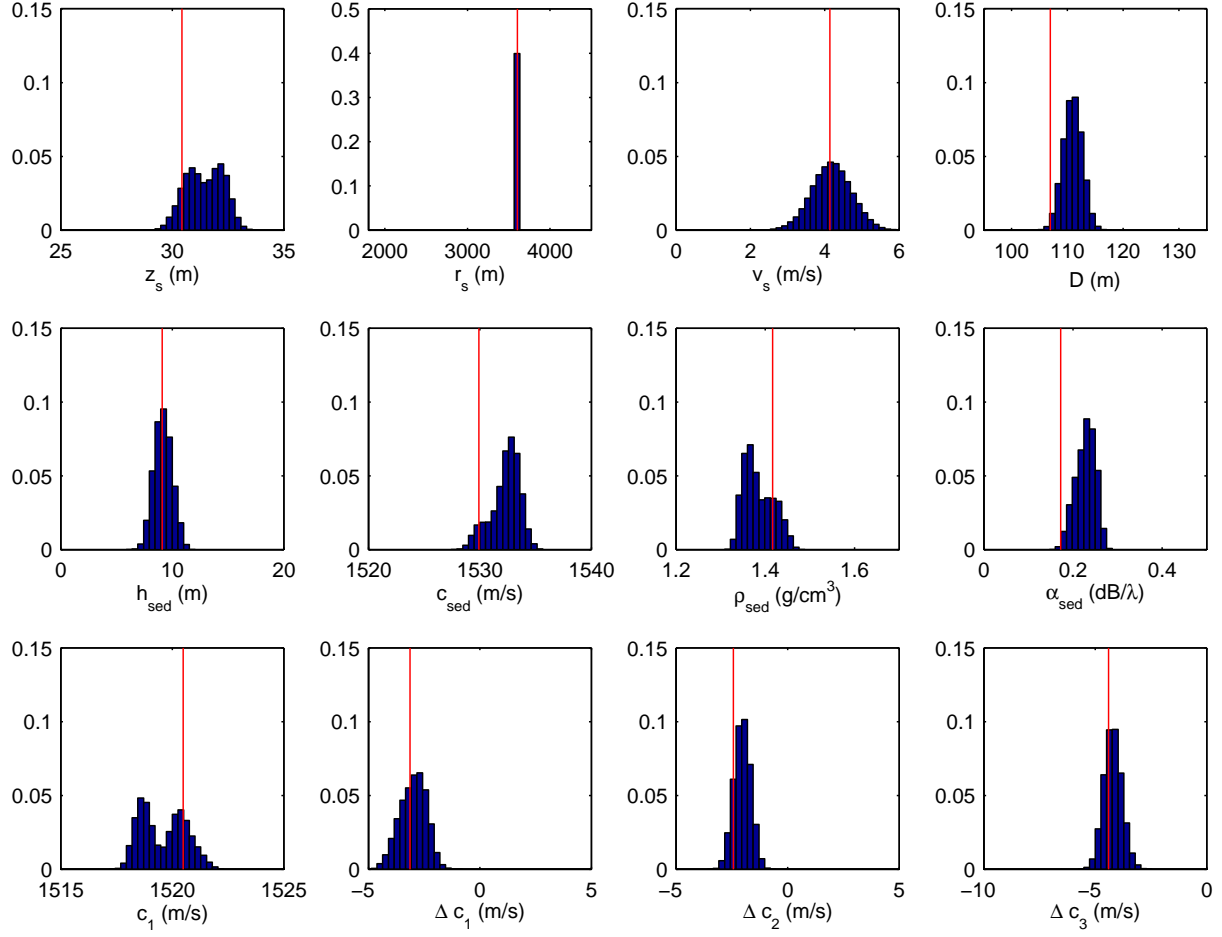


FIG. 3. (Color online) Histograms of the particles showing the 1-D PPD of all source and environmental parameters at $t = 10$ min. Vertical lines show the true values.

even though the environmental state equation expects the environment to be the same from one step to another, $E(\mathbf{m}_{k+1}) = E(\mathbf{m}_k)$. Nevertheless, when the depth D is rapidly varying, the marginal PPD (Fig. 3) lags slightly the true value and the current PF with constant environment assumption is barely able to keep up with the fast changes at each step.

The primary goal is to track the moving source, hence the environmental track needs only to be sufficient to perform accurate source tracking². The full PF can track all of the source parameters almost perfectly for this simulation. As the PF can operate with any PDF, it is a good choice for the variety of densities observed in Fig. 3.

Evolution of the 2-D PPDs for some environmental parameter couplings Δ at three time

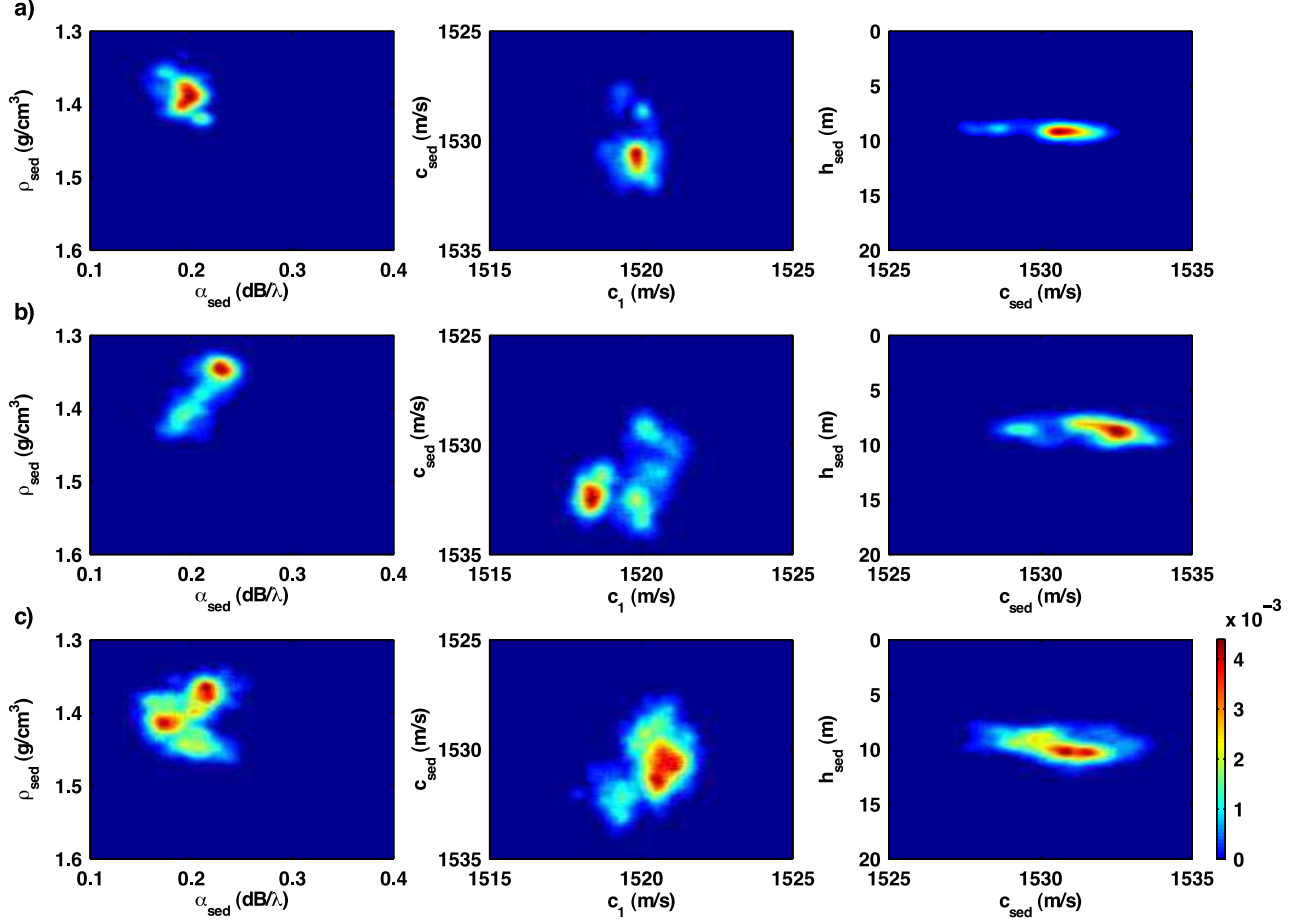


FIG. 4. (Color online) Various 2-D PPDs at time (a) 5 min, (b) 10 min, and (c) 13.3 min.

steps are given in Fig. 4. The 2-D $\alpha_{sed} - \rho_{sed}$ PPD starts as a unimodal Gaussian density and first the Gaussian shape is lost, then a tail density with a strong parameter correlation is formed, finally evolving into a complex, multimodal PPD. The 2-D $c_1 - c_{sed}$ PPD also exhibits similarly complex PPDs and PPD evolutions. The 2-D $c_{sed} - h_{sed}$ PPD shows a narrow, relatively unimodal PPD with a small variance in h_{sed} and a large one in c_{sed} . Similar to the 1-D PPDs, the 2-D PPDs become wider and uncertainty increases as time increases. Although not shown here, this decrease in the track quality is largely due to the decreasing SNR as the ship moves away.

The evolution of the 2-D PPD of the source depth/range (also referred as the posterior source ambiguity surface¹⁷) at three time steps is given in Fig. 5. The ability to track both

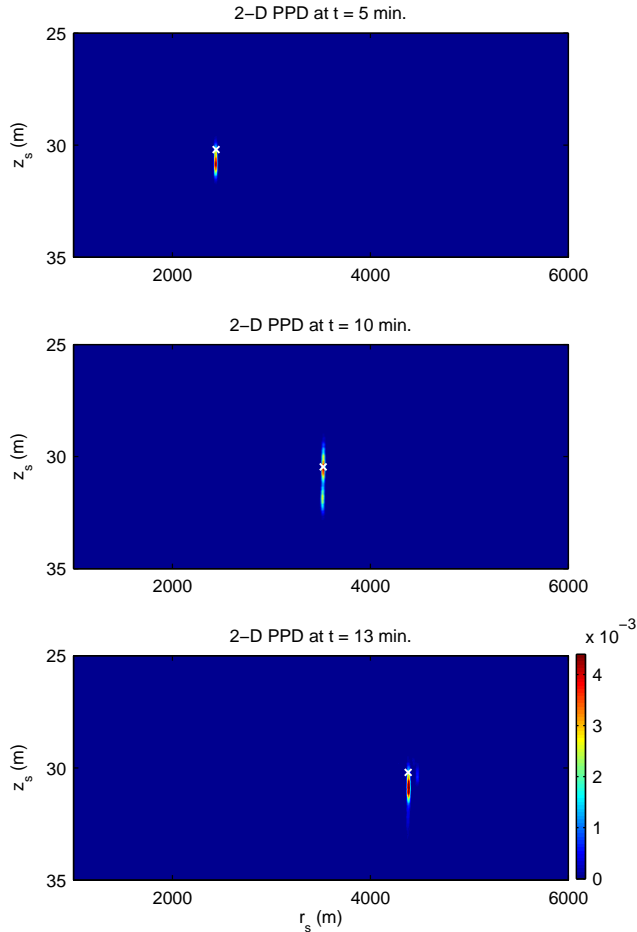


FIG. 5. (Color online) 2-D depth-range PPD of the moving source at time $t = 5, 10$, and 13.3 min. \times represents the true source location.

the environment and the source enables the full PF to accurately track the source with a small variance both in range and depth. The results at the mid point and the end of the track are given in Table III. The full PF makes only 0.1 m, 1 m, and less than 0.1 m/s error at the mid-track for the source depth, range, and speed, respectively. Even after the full track length of 13.3 min., the error terms stay at 0.6 m, 2 m, and 0.1 m/s.

The main purpose of the current selection of changes in the ocean parameters is to test the abilities of the PF under conditions that are known to create large errors in MFP source localization. The error made both in source range and depth estimation when the change in water depth is not included in the MFP is well-studied^{21,22}. When there is a

mismatch between the assumed water depth and its actual value, the source appears at a different location which is known as the source mirage effect. Therefore, the bathymetry changes from initially flat (at 130 m) to a sloped-bottom as the ship moves into shallower water finally reaching a water depth of 100 m at the source location. This way, a mirage is formed after $t = 0$ and it slowly moves away from the true location if the environment is assumed constant. Fig. 6 shows the output of such a mismatched MFP estimator that uses a normalized Bartlett mismatch in dB:

$$B(\mathbf{m}_k) = 1 - \frac{1}{n_f} \sum_{j=1}^{n_f} \frac{|[\mathbf{h}^j(\mathbf{m}_k)]^H \mathbf{y}_k^j|^2}{|\mathbf{y}_k^j|^2 |\mathbf{h}^j(\mathbf{m}_k)|^2}. \quad (18)$$

In an ideal waveguide with pressure release boundaries, the ratio of MFP range estimate to true source range is equal to the ratio of flat bathymetry water depth to true water depth at source location, creating a mirage²². The same ratio is valid for source depth regardless of the frequency used. Since the actual environment used here is more complex with a sedimentary layer these relations are approximate. Nevertheless, a mirage is formed 637 m further away and 14.5 m deeper than the true source at $t = 13.3$ min (\times in Fig. 6(b)).

To show that the inclusion of the environmental parameters improves tracking of the source location, a source-only PF is used with the environment at $t = 0$ (\diamond in Fig. 6). This PF tracks the slowly diverging mirage with a posterior value close to the mismatched-MFP maxima at all times, see Fig. 6(b). In contrast, the full PF tracks the true source range and depth for all t .

The evolution of the three source parameters are given in Fig. 7. The slowly diverging mirage clearly can be observed. Note how the source-only PF has a fluctuating source speed to be able to track the mirage in the evolving environment. On average, the mirage moves faster and deeper than the true source for this environment and hence both the range error and depth error between the source-only PF and the full PF increase with time.

It is interesting to note that, by running the source-only and full PF together it is possible to track both sources and mirages and rate of change of the error between them. This provides an estimate for the rate at which one must perform a geoacoustic inversion

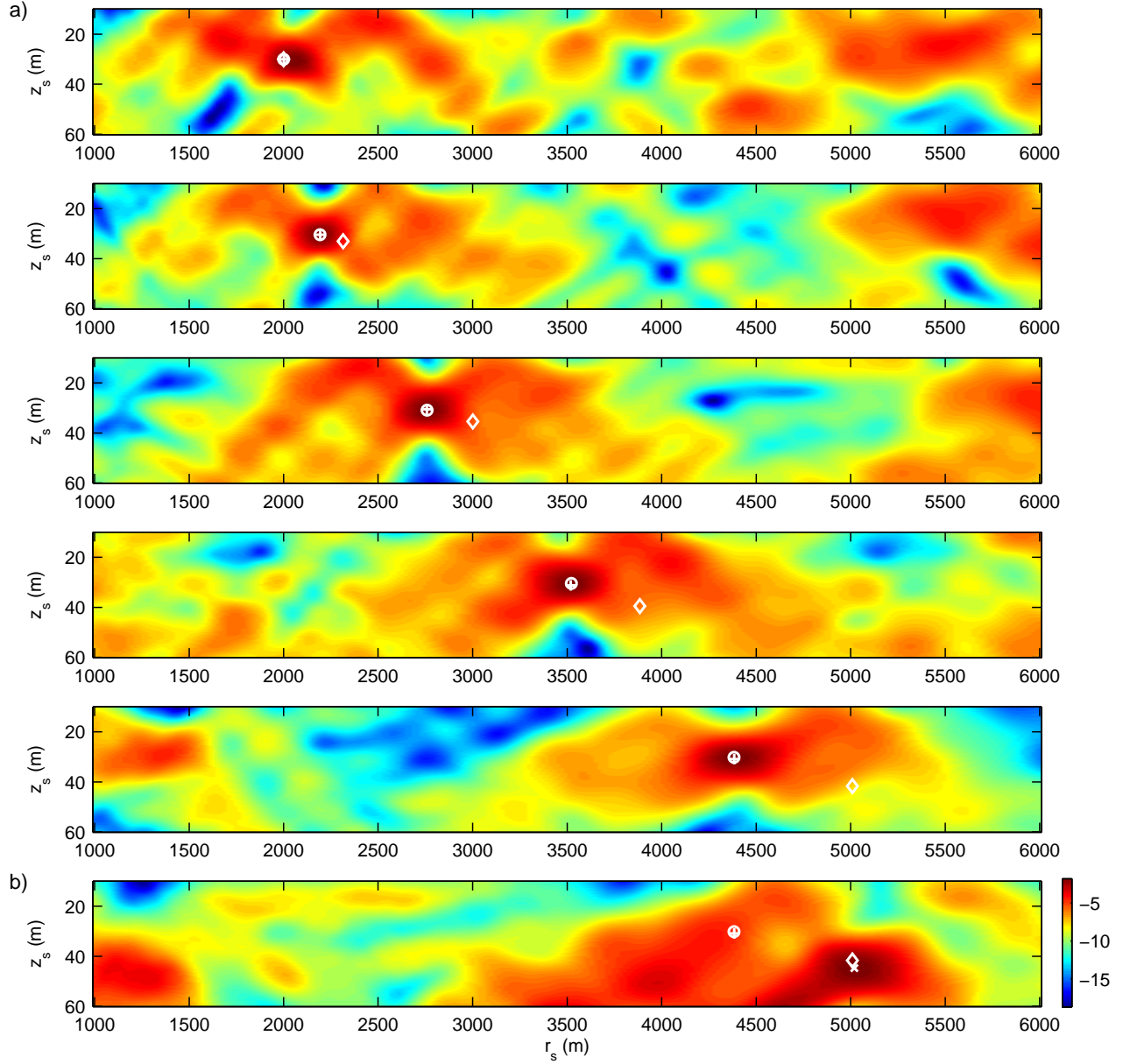


FIG. 6. (Color online) (a) Comparison between the source-only PF (\diamond) and full PF ($+$) at $t = 0, 3.3, 6.7, 10, 13.3$ min ($k = 0, 10, 20, 30, 40$), respectively. Background is the MFP source location ambiguity surface for the true environment. ‘o’ is the true source location. (b) Results at $t = 13.3$ min. where the background is the mismatched-MFP that uses a constant environment (at its $t = 0$ value). ‘x’ shows the maximum of the mismatched-MFP where the mirage is located.

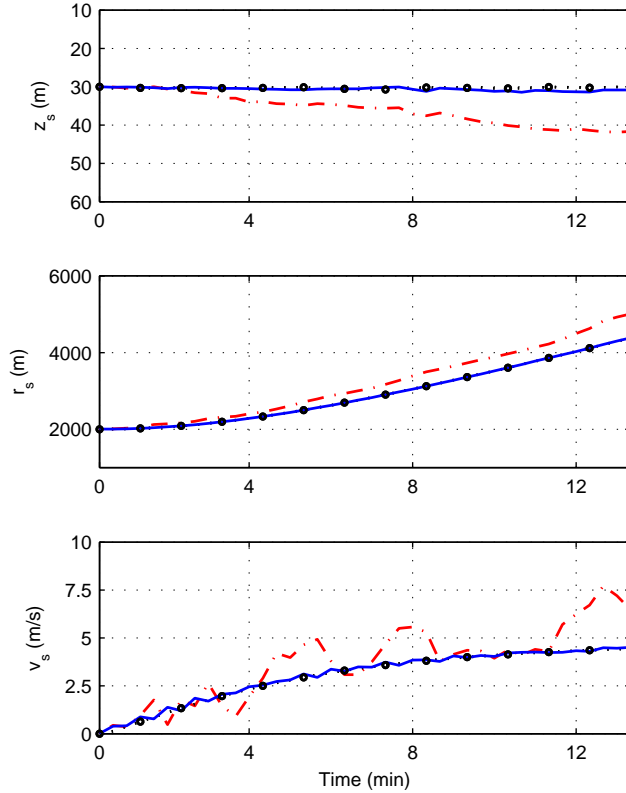


FIG. 7. (Color online) Track results of three source parameters for full PF (solid) vs. source-only PF (dashed), together with the true trajectory ('o').

to update the current values of the environmental parameters in order to successfully track the source using conventional source tracking algorithms.

V. SUMMARY

A particle filtering (PF) approach has been presented for passively tracking a moving acoustic underwater source in a changing ocean acoustic environment. This approach treats both the environmental and acoustic source parameters as unknown random variable that change in time. Inclusion of environmental parameters in the PF reduces the environmental mismatch that result in significant errors in matched field processing. The need to analyze the sequential stream of acoustic data in real-time, the nonlinearity between the source/environmental parameters and the measured acoustic field, and the non-Gaussian

posterior probability densities (PPD) typically encountered in geoacoustic inversions makes sequential Monte Carlo techniques an attractive complement to other techniques used in underwater source tracking.

The geoacoustic PF is able to track the environmental and source parameters together with their underlying uncertainties in the form of a space and time evolving PPD. The capabilities of the algorithm were demonstrated in simulation for an environment with evolving water depth, sound speeds, density and attenuation values, and sediment thicknesses. The water depth mismatch resulted in the well-known source mirage effect but the PF still was able to track the true source, geoacoustic parameters, and their evolving densities in this space and time varying environment.

VI. ACKNOWLEDGMENT

This work was supported by the Office of Naval Research, under grant numbers N00014-05-1-0264 and N00014-09-1-0313.

References

TABLE I. Environmental parameters.

	\mathbf{x}	\mathbf{x}_0	$\mathbf{P}_0^{1/2}$	State noise, $\mathbf{Q}_k^{1/2}$	L. Bound	U. Bound
Source	z_s (m)	30	0.2	0.2	1	100
	r_s (m)	2000	50	$0.025 \times \frac{\Delta t^2}{2}$	500	8000
	v_s (m/s)	0	0.01	$0.025 \times \Delta t$	0	10
Water	c_1 (m/s)	1520	0.15	0.15	1515	1525
	Δc_1 (m/s)	-3	0.15	0.15	-5	5
	Δc_2 (m/s)	-2	0.15	0.15	-5	5
	Δc_3 (m/s)	-5	0.15	0.15	0	10
	D (m)	130	0.8	0.8	80	150
Sediment	c_{sed} (m/s)	1530	0.25	0.25	1450	1600
	h_{sed} (m)	9	0.25	0.25	0	30
	ρ_{sed} (g/cm ³)	1.4	0.005	0.005	1	1.7
	α_{sed} (dB/ λ)	0.2	0.005	0.005	0	1
Bottom	c_{bot} (m/s)	1570	-	-	1550	1650
	ρ_{bot} (g/cm ³)	1.6	-	-	1	2
	α_{bot} (dB/ λ)	0.2	-	-	0	1

TABLE II. Simulation parameters.

Receiver type	VLA	Source frequencies	200, 275, 350, 425 Hz
No. of hydrophones	24	SNR at $r = 2.0$ km (\mathbf{R}_0)	8.8 dB
Array start depth	26 m	SNR at $r = 4.4$ km (\mathbf{R}_{40})	3.1 dB
Array end depth	118 m	Track length	13.3 min. ($k = 40$)
PF size	10,000	Sampling interval, Δt	20 s
Water depth at receiver array	130 m	Source velocity	5 m/s

TABLE III. Results.

t (min)	Method	z_s (m)	r_s (m)	v_s (m/s)
6.7	True value	30.6	2691	3.3
	Full PF	30.5	2690	3.3
	Mismatched MFP	35.7	2941	–
	Source-only PF	34.9	2934	3.1
13.3	True value	30.2	4383	4.4
	Full PF	30.8	4385	4.5
	Mismatched MFP	44.7	5020	–
	Source-only PF	41.7	5009	6.5

List of Figures

FIG. 1	(Color online) (a) Geoacoustic model used in the simulations, (b) the simulation set-up involving a fixed VLA and moving source in a range-dependent environment, and (c) sensitivity plots of geoacoustic parameters at $t = 0$	11
FIG. 2	(Color online) Time evolving marginal posterior density for the full PF simulation and the true trajectory (solid white) of each parameter.	14
FIG. 3	(Color online) Histograms of the particles showing the 1-D PPD of all source and environmental parameters at $t = 10$ min. Vertical lines show the true values.	15
FIG. 4	(Color online) Various 2-D PPDs at time (a) 5 min, (b) 10 min, and (c) 13.3 min.	16
FIG. 5	(Color online) 2-D depth-range PPD of the moving source at time $t = 5, 10,$ and 13.3 min. \times represents the true source location.	17
FIG. 6	(Color online) (a) Comparison between the source-only PF (\diamond) and full PF (+) at $t = 0, 3.3, 6.7, 10, 13.3$ min ($k = 0, 10, 20, 30, 40$), respectively. Background is the MFP source location ambiguity surface for the true environment. ‘o’ is the true source location. (b) Results at $t = 13.3$ min. where the background is the mismatched-MFP that uses a constant environment (at its $t = 0$ value). ‘ \times ’ shows the maximum of the mismatched- MFP where the mirage is located.	19
FIG. 7	(Color online) Track results of three source parameters for full PF (solid) vs. source-only PF (dashed), together with the true trajectory (‘o’).	20